Microfluidic Synthesis of Macroporous Copolymer Particles

Stanislav Dubinsky,[†] Hong Zhang,[†] Zhihong Nie,[†] Ilya Gourevich,[†] Dan Voicu,[†] Martin Deetz,[‡] and Eugenia Kumacheva*,[†]

Department of Chemistry, University of Toronto, 80 Saint George Street, Toronto, Ontario M5S 3H6, Canada, and Rohm and Haas Chemicals, LLC, 727 Norristown Road, Spring House, Pennsylvania 19477-0904

Received February 8, 2008; Revised Manuscript Received March 14, 2008

ABSTRACT: Macroporous copolymer particles have a broad range of applications such as ion exchange resins and sorbents, catalyst supports, and carriers of biologically active species. Many of these applications require precise control of the dimensions of microbeads in the range from 50 to 100 μm and predetermined size of pores. This paper reports semicontinuous photoinitiated microfluidic synthesis of macroporous polymer particles with the designated dimensions and a range of internal structures. Comparison with microspheres synthesized by conventional suspension polymerization shows that microfluidic synthesis provides better control over the porous structure of the microbeads.

1. Introduction

Macroporous polymer resins are a class of materials with a permanent well-defined porous structure.[1] A broad range of applications of these polymers includes their use as ion exchange resins and sorbents,[2] catalyst supports,[1] and materials for biomedical applications.[3−10] In particular, in the latter group of the applications, copolymer networks serve for the immobilization of enzymes,[3] tissue engineering,[4] protein separation,[5] embolization,[6−8] blood plasma detoxification,[9] and the controlled release of pharmaceuticals.[10]

The methods developed for the production of rigid macroporous polymers can be tentatively divided into two groups: the synthesis of macroscopic monolithic materials and the synthesis of particulate materials.[11−22] Rigid macroporous polymer monoliths show advantages over particulate materials in high-throughput separation processes and in catalytic reactions;[11−16] however, problems such as the initial high flow resistance and breakthrough curve aberrations have been incurred in the operation of these materials.[5] In addition, polymeric monoliths are currently not amenable to large column formats. As a result, packed bed columns currently dominate in preparative chromatography.[23]

Particulate macroporous resins are obtained by milling macroscopic materials to form irregular particles that are subsequently fractionated to narrow their size distribution.[5,19] Although easy to prepare, these particles are poorly packed in columns and due to the presence of tiny secondary particles may clog the system.[19] Alternatively, polymer macroporous particles are produced by heterogeneous polymerization techniques.

Suspension polymerization is generally used for the synthesis of microspheres with a diameter in the range from 0.1 to 1.5 mm and a relatively broad size distribution.[2,24a]

In this method, droplets of a monomer, an initiator, and an inert solvent (porogen) are dispersed in the immiscible continuous phase by using stirring, jetting, sonication, or homogenizing techniques. The porogen is miscible with the monomer but is immiscible with the polymer phase. Following polymerization of the particles, the porogen and residual monomers are extracted with a solvent or removed by steam distillation, leaving behind a network of pores. Generally, particles with dimensions below 200 μm have a broad range of sizes, mostly because of the insufficient control of the emulsification process and coalescence of droplets in the polymerization stage.

Macroporous polymer highly monodispersed particles with dimensions below 50 μm are typically prepared by the seeded emulsion polymerization method. Swelling of monodisperse latex particles (seeds) with a solvent and monomers followed by the polymerization of the monomer and the removal of the immiscible solvent yields macroporous particles with a narrow size distribution.[17,18,20,21] Using seed particles with a low cross-linking density favors their rapid swelling; however, the procedure is time-consuming, especially for the synthesis of particles with dimensions exceeding 100 μm.

Macroporous particles with diameters below 10 μm have been also obtained by the precipitation polymerization in organic solvents. For example, toluene and xylene have been used as cosolvents with acetonitrile to produce monodispersed, highly cross-linked divinylbenzene particles.[22]

The size, the shape, and the distribution of sizes are vital in many applications of macroporous particles. Polydisperse microbeads show reduced performance in chromatographic applications due to the band broadening and increased column back-pressure.[22] Irregularly shaped particles are susceptible to mechanical attrition and breakdown into debris.[1] Small interparticle void space results in increased column back-pressure. Although macroporous particles obtained by heterogeneous polymerization techniques are primarily spherical, the existing methods are material- and size-specific. In addition, further fractionation is often required to narrow particle size distribution.[1]

The size of pores in the particles is another important factor in the synthesis of macroporous beads, which is controlled by varying the type and the amount of porogen and cross-linker and by tuning polymerization temperature.[1,2,24b] A broad range of applications of macroporous copolymers requires a "tailor-made" pore size and pore size distribution. For instance, microbeads used in the size exclusion chromatography of oligomers and small molecules require pore size on the order of 100 Å,[25,26] whereas protein separation and catalyst support require materials with a size of pores up to 4000 Å, to ensure unrestricted diffusion of the dissolved substances into the polymer and back into the surrounding solution.[25]

A method that yields monodispersed macroporous particles with dimensions in the range from 50 to 100 μm along with

* Corresponding author.
[†] University of Toronto.
[‡] Rohm and Haas Chemicals.

10.1021/ma800300d CCC: $40.75
Published on Web 05/03/2008

control over the size of pores is highly desirable. Recently, microfluidic syntheses allowed for the production of polymer particles, with controlled sizes, shapes, and internal structures and extremely narrow size distribution.[27–30] The ability to generate porous particles by means of microfluidic synthesis has been demonstrated,[27] yet currently no thorough study exists on the formation of macroporous particles with predetermined dimensions and controlled pore size distribution. Here we report semicontinuous photoinitiated microfluidic synthesis of macroporous polymer particles with a narrow size distribution in the size range from tens to a hundred micrometers. The microbeads were synthesized by (i) emulsification of the mixture of glycidyl methacrylate (GMA), ethylene glycol dimethacrylate (EGDMA), and a porogen in the microfluidic droplet generator; (ii) on-chip photopolymerization of GMA-*co*-EGDMA copolymer; and (iii) off-chip post-photopolymerization of poly(GMA-*co*-EGDMA). The use of GMA was motivated by the ability to carry out subsequent surface modification of the resulting microbeads due to the reactivity of the pendant epoxide groups.[19] Combination of the advantages of conventional suspension polymerization and microfluidic synthesis allowed us to produce polymer particles with a narrow size distribution and a controlled size of pores.

2. Experimental Section

Materials. Monomers glycidyl methacrylate (GMA) and ethylene glycol dimethacrylate (EGDMA), photoinitiators 2,2-dimethoxy-2-phenylacetophenone (DMPA), 2-hydroxy-2-methylpropiophenone (HMPP), and 1-hydroxycyclohexyl phenyl ketone (HCPK), porogen solvents diethyl phthalate (DEP), diisobutyl phthalate (DBP), dioctyl phthalate (DOP), and diisodecyl phthalate (DDP), and a stabilizer poly(vinyl alcohol), 87−89% hydrolyzed with $M_w \sim 13\,000-23\,000$ (PVA), were purchased from Aldrich Canada and used as received. SU-8 50 photoresist was purchased from MicroChem. Prepolymer Sylgard 184 Silicon was supplied as a two-part kit by Dow Corning Corp. Polyethylene tubing was purchased from Becton Dickinson.

The appropriate photoinitiator was selected by examining conversion of monomer-to-polymer in free-radical polymerization reactions conducted with several photoinitiators. A GMA−EGDMA mixture mixed with DMPA, HCPK, or HMPP was exposed to UV irradiation for the time intervals varying from 15 to 200 s. The highest reaction rate (ca. 100% conversion in 60 s) was obtained when using DMPA. In the microfluidics synthesis to ensure complete polymerization, we conducted 60 s on-chip polymerization and 180 s off-chip postpolymerization of the particles. (Postpolymerization was required because the material of the microfluidic reactor partly absorbed UV light during the microfluidic synthesis.)

Microfluidic Synthesis. Microfluidic reactors for the synthesis of macroporous particles were fabricated in poly(dimethylsiloxane) by using a standard soft-lithography method.[31] Masters were prepared using an SU-8 photoresist (MicroChem) in bas-relief on silicon wafers.

Figure 1a shows a schematic of the individual microfluidic reactor. The reactor contains the emulsification compartment (1), on-chip photopolymerization compartment (2), and off-chip photopolymerization compartment (not shown in the figure). Figure 1b shows a zoomed in schematic of the emulsification compartment (1): a three-channel microfluidic flow-focusing droplet generator.[32] Two immiscible liquids (the monomer mixture, liquid A, and the continuous phase, an aqueous 3 wt % solution of PVA, liquid B) were supplied to the microchannels and forced into the narrow orifice, as shown in Figure 1b. In the present work, the monomer mixture comprised 27 wt % GMA, 18 wt % EGDMA, 55 wt % of the porogen (e.g., DEP, DBP, DOP, or DDP) (corresponding to 53.8, 55.6, 57.3, and 57.4 vol %, respectively), and 4.5 wt % of photoinitiator DMPA (based on the total mass of the reaction mixture). In the orifice or slightly behind the orifice, a thread of the monomer mixture (liquid A) broke up and released droplets. The droplets were exposed to UV irradiation in the polymerization compartment—an extension wavy channel with the width of 600 μm and the length of 125 mm. Photopolymerization was carried out in the microfluidic reactor for ca. 60 s. Following on-chip polymerization, the particles were collected in the glass vial and postpolymerized under UV irradiation for another 180 s. Both polymerization processes were conducted under UV light ($I = 200$ mW/cm^2, $\lambda = 360$ nm, Honle UV Technology). The distance between the lamp and the microfluidic chip was 15−20 cm. Following polymerization, the porogen liquids were removed by washing the microbeads in methanol and acetone.

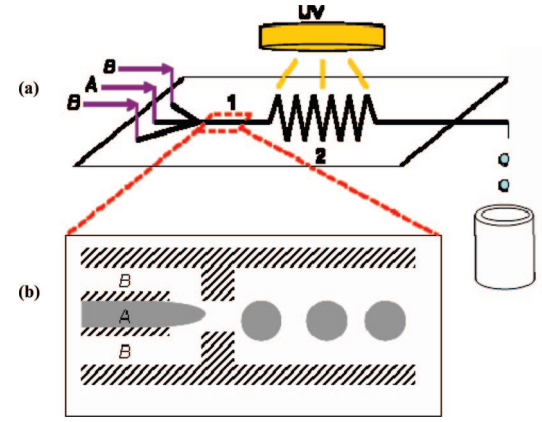

Figure 1. (a) Schematic of the continuous microfluidic reactor: (1) emulsification compartment, (2) on-chip polymerization compartment. (b) Zoomed-in emulsification compartment. A: a monomer mixture. B: a 3 wt % aqueous solution of PVA (continuous phase).

Table 1. Solubility Parameters of the Solvents Used for the Determination of the Solubility Parameter of Poly(GMA-*co*-EGDMA)[a]

solvents	solubility parameter,[a] (MPa)$^{1/2}$	solvents	solubility parameter,[a] (MPa)$^{1/2}$
acetaldehyde	21.1	ethanol	26.0
N,N-dimethylacetamide	22.8	methanol	29.7
acetonitrile	24.3	glycerol	33.8
N,N-dimethylformamide	24.8		

[a] The values of solubility parameters of solvents were acquired from ref 33.

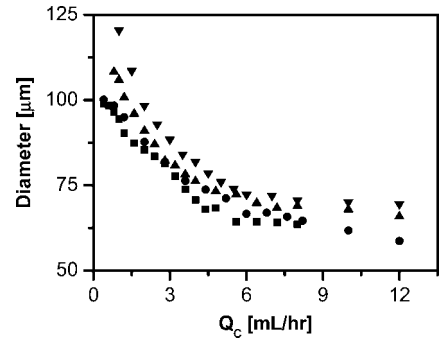

Figure 2. Variation in the size of droplets of DEP−monomer mixture plotted as a function of the flow rate, Q_c, of the continuous aqueous phase. Flow rates of the monomer mixture, Q_m: (■) 0.02, (●) 0.05, (▲) 0.10, and (▼) 0.40 mL/h.

In the series of control experiments, macroporous particles were obtained via conventional photoinitiated suspension polymerization of droplets with the compositions identical to those used in microfluidic synthesis in an aqueous 3 wt % solution of PVA. Droplets were obtained using microfluidic emulsification, transferred into a vial, and polymerized for 5 min.

Particle Characterization. The distributions of the sizes of droplets and of the corresponding macroporous particles were determined by image analysis of optical microscopy images using

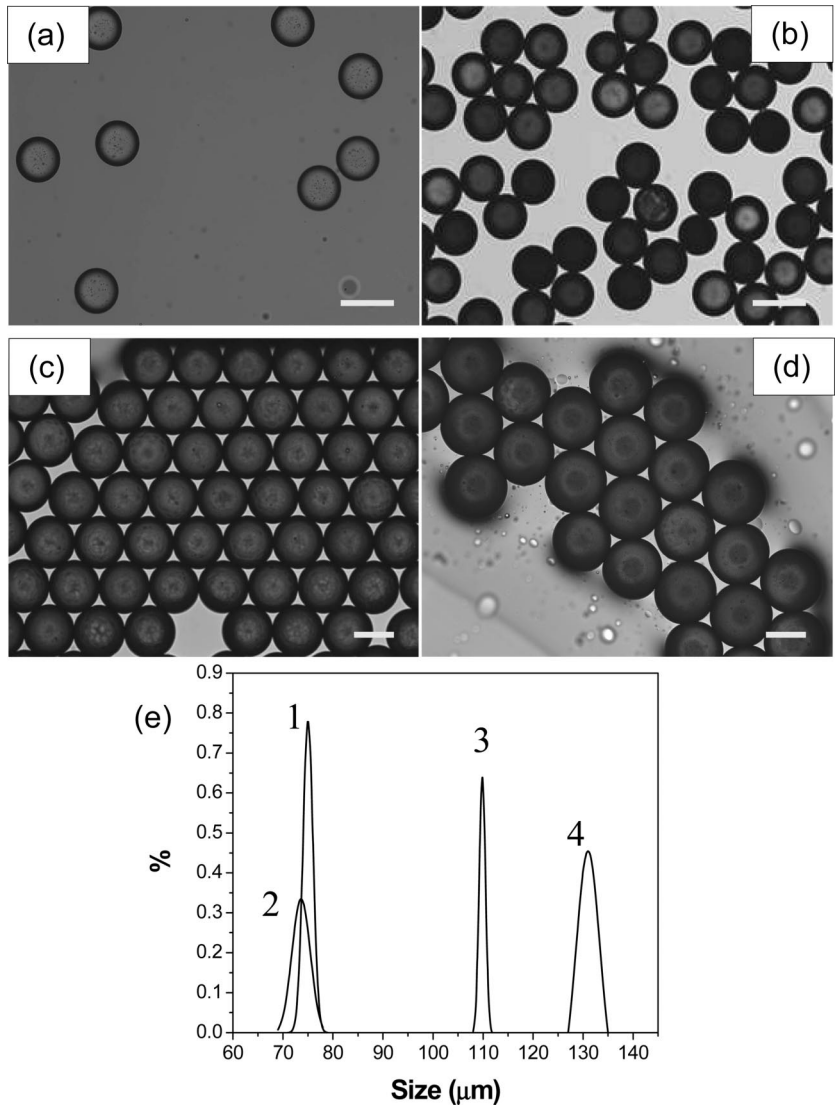

Figure 3. Optical microscopy images of poly(GMA−EGDMA) particles after 60 s on-chip polymerization and 180 s off-chip polymerization of monomer mixtures comprising DEP (a), DBP (b), DOP (c), and DDP (d). Scale bar is 100 μm. (e) Size distribution of particles prepared using different porogen solvents: (1) DEP, $Q_m = 0.08$ mL/h, $Q_c = 4.2$ mL/h; (2) DBP, $Q_m = 0.08$ mL/h, $Q_c = 4.2$ mL/h; (3) DOP, $Q_m = 0.1$ mL/h, $Q_c = 1.5$ mL/h; (4) DDP, $Q_m = 0.1$ mL/h, $Q_c = 1.2$ mL/h.

the Image Pro (Media Cybernetics) software. Generally, 200 droplets or 100 particles were examined to determine the coefficient of variation (CV) of their dimensions, defined as the ratio of standard deviation in droplet (particle) size to the mean diameter.

The internal structure of particles was examined in scanning electron microscopy (SEM) experiments that were carried out on the Hitachi S-5200 electron microscope at the accelerating voltage of 1−2 kV. A droplet of particle dispersion was placed onto the copper grid coated with carbon (Electron Microscope Sciences Inc.) and allowed to dry. The specific surface areas were determined by measuring the adsorption and desorption isotherms of nitrogen on a Quantachrome AS1C-VP2 apparatus with a bath temperature of 77 K and evaluated using BET equation.

Internal porous structure of the particles was also verified using scanning confocal microscopy (Leica TCS SP2) with a 20× dry objective, NA = 0.5 at $\lambda_{ex} = 488 \pm 20$ nm and $\lambda_{em} = 525 \pm 25$ nm. Prior to the characterization, the macroporous particles were immersed for 12 h into the 0.01 mM aqueous solution of the fluorescent dye Rhodamine 6G (Rh6).

Conversion of monomer mixtures was determined in FTIR experiments conducted on films by monitoring the change in the ratio of the intensity of two absorption peaks centered at 1620 cm^{-1} (C═C stretching) and at 810 cm^{-1} (C═C−H bending) to the intensity of the reference absorption peak located at 1720 cm^{-1} (C═O stretching) in the course of the polymerization process (exemplary FTIR spectra are presented in the Supporting Information).

The value of the solubility parameter of poly(GMA-*co*-EGDMA) was obtained by determining the swelling of polymer films in different solvents. The list of solvents and the corresponding solubility parameters are given in Table 1.

3. Results

Figure 2 shows the variation in the sizes of droplets of monomer−DEP mixture plotted as a function of the flow rate of the continuous aqueous phase, Q_c, for the different flow rates of the monomer mixture, Q_m. Emulsification of the reaction mixture yielded droplets with the diameter in the range from 55 to 150 μm. In the entire range of flow rates of the liquids, the droplets formed in the flow-focusing regime[32] and their polydispersity did not exceed 3%. When the flow rate of the continuous aqueous phase increased from 1.5 to 12 mL/h, the diameters of droplets reduced from 120 to 40 μm, respectively. Generally, with the increasing flow rate of the monomer phase (for the invariant flow rate of the aqueous phase) the size of droplets increased. Qualitatively similar results were obtained in the emulsification of monomer mixtures comprising DBP,

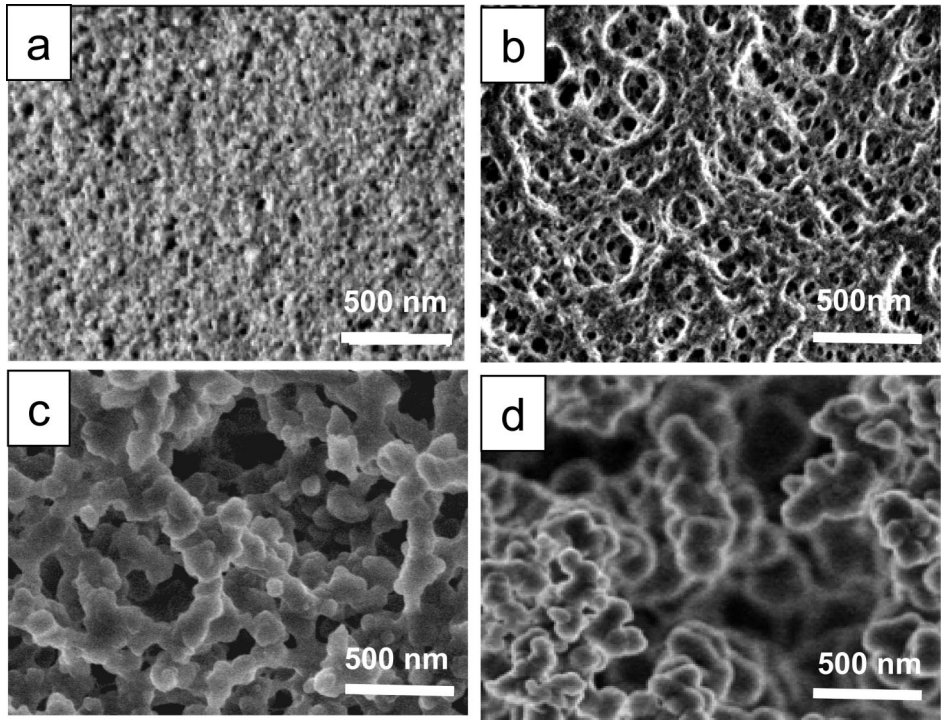

Figure 4. SEM images of the surface of macroporous particles obtained by polymerizing monomer mixtures comprising (a) DEP, (b) DBP, (c) DOP, and (d) DDP porogens. The emulsification was carried at flow rates of liquids specified in Figure 3.

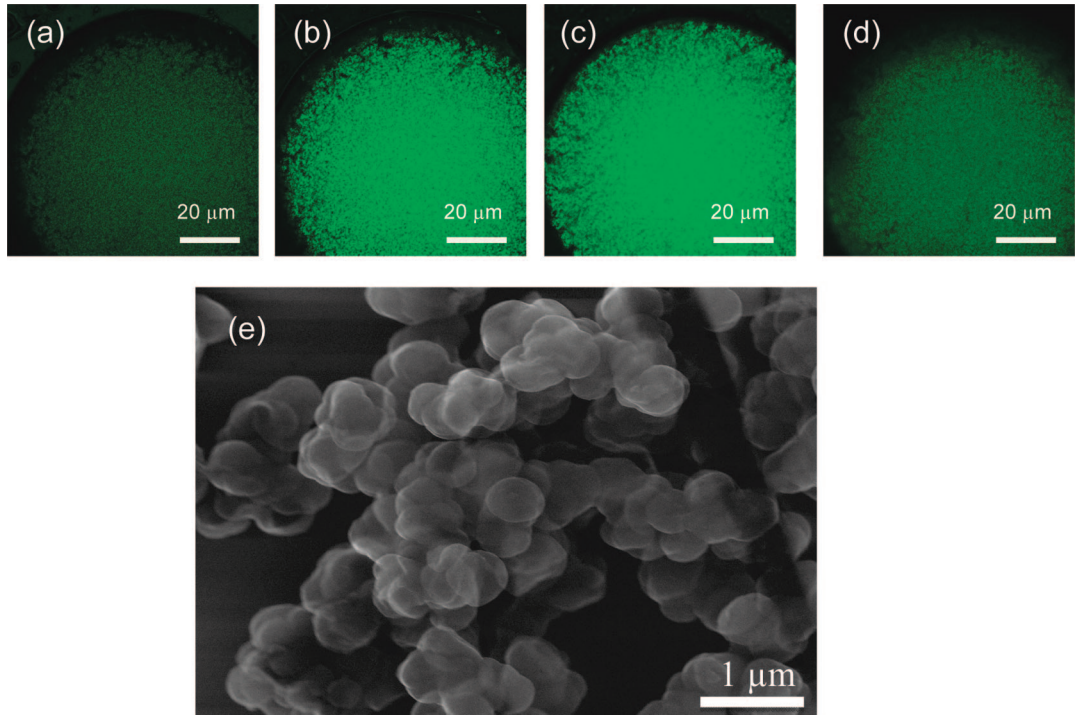

Figure 5. (a−d) Confocal microscopy images of DOP-based particle acquired by imaging the microbead with diameter of ca. 110 μm along the *Z*-axes starting from the depth of 13 μm with the step of 10 μm between images. (e) SEM image of microtomed particle derived from the DOP−monomer mixture, as in Figure 4c.

DOP, and DDP porogens, although typically, the size of droplets decreased when the droplet phase contained a more polar porogen.

When the flow rate of the monomer phase exceeded 1 mL/h and the ratio of the flow rates of the continuous-to-droplet phases exceeded 25, a transition occurred from the flow-focusing to the jetting emulsification regime. Typically, polydispersity of the droplets generated in the jetting regime was 8−12%, excluding small "satellite" droplets which accompanied the main population of droplets.

The droplets moved to the polymerization compartment of the microfluidic reactor where they were exposed to UV irradiation. In the polymerization microchannel the droplets were separated by the well-defined distance of ca. 1 mm; hence, their coalescence was suppressed. Following on-chip polymerization, the particles were postpolymerized off-chip.

Table 2. Properties of Macroporous Poly(GMA-*co*-EGDMA) Particles Shown in Figures 3–5

sample	1	2	3	4
porogen	DEP	DBP	DOP	DDP
mean particle diameter,[a] μm	75	74	110	131
$CV_{particle}$,[a] %	1.00	2.95	0.83	2.70
specific surface area,[b] m^2/g	28.7	13.9	6.6	3.4

[a] Obtained by analyzing optical microscopy images. [b] Obtained by the BET method.

Table 3. Solubility Parameters of the Porogen Solvents, the Monomers, and the Corresponding Polymer

chemicals	solubility parameter, $(MPa)^{1/2}$	chemicals	solubility parameter, $(MPa)^{1/2}$
DEP	20.5[33]	GMA	18.2[35]
DBP	19.0[33]	EGDMA	18.2[36]
DOP	16.2[33]	poly(GMA-*co*-EGDMA)	~24[a]
DDP	14.7[33]		

[a] Experimentally found.

Figure 3a−d shows optical microscopy images of the resulting particles after extracting the porogen. All particles had a narrow particle size distribution (Figure 3e); thus, we conclude that the narrow size distribution of the droplets was preserved due to their on-chip prepolymerization. The surface of the microbeads had a well-defined porous structure, as shown in Figure 4a−d, dependent on the type of porogen used.

The presence of the porous structure *in the interior* of the particles was verified in both SEM experiments conducted for the microtomed particles and in the confocal fluorescence microscopy (CFM) experiments. Figure 5a−d shows a series of exemplary images of the 110 μm size particle synthesized by polymerizing the monomer−DOP mixture and infiltrated with an aqueous solution of the Rhodamine 6G dye. The images were collected along the *Z*-direction with the step of 10 μm, starting from the depth of 13 μm. Because of the presence of the interconnected network of pores, the solution of a fluorescent dye infiltrated the entire body of the particle. An SEM image in Figure 5e shows a well-defined porous structure of the microtomed particle synthesized from the DOP−monomer mixture, as shown in Figure 3c.

Table 2 summarizes the properties of particles shown in Figures 3 and 4. All particles had coefficient of variation (CV) below 3% regardless of the microbead size. The specific surface area (related to the size of pores) of the microbeads increased in the row DDP → DOP → DBP → DEP. In order to explain the effect of the nature of porogen on the size of pores in the macroporous beads, we compared the solubility parameters of the porogen liquids, the monomers GMA and EGDMA, and poly(GMA−EGDMA).

Table 3 shows that the porogens DBP and DEP had the solubility parameters that were close to that of the poly(GMA−EGDMA) mixture. These porogens yielded particles with smaller pores, presumably due to the dominant role of the v-induced syneresis in the process of formation of pores.[34] In this mechanism, a thermodynamically "good" porogen is used and the growing polymer gel collapses and forms nuclei,[2] whereas the porogen and the rest of the monomers remain in the continuous phase of the reaction mixture. As the polymerization and cross-linking processes proceed, new nuclei form and agglomerate in small globules, yielding a structure with small pores. The porogens DOP and DDP had substantially lower values of solubility parameters than poly(GMA-*co*-EGDMA). During polymerization, because of the greater

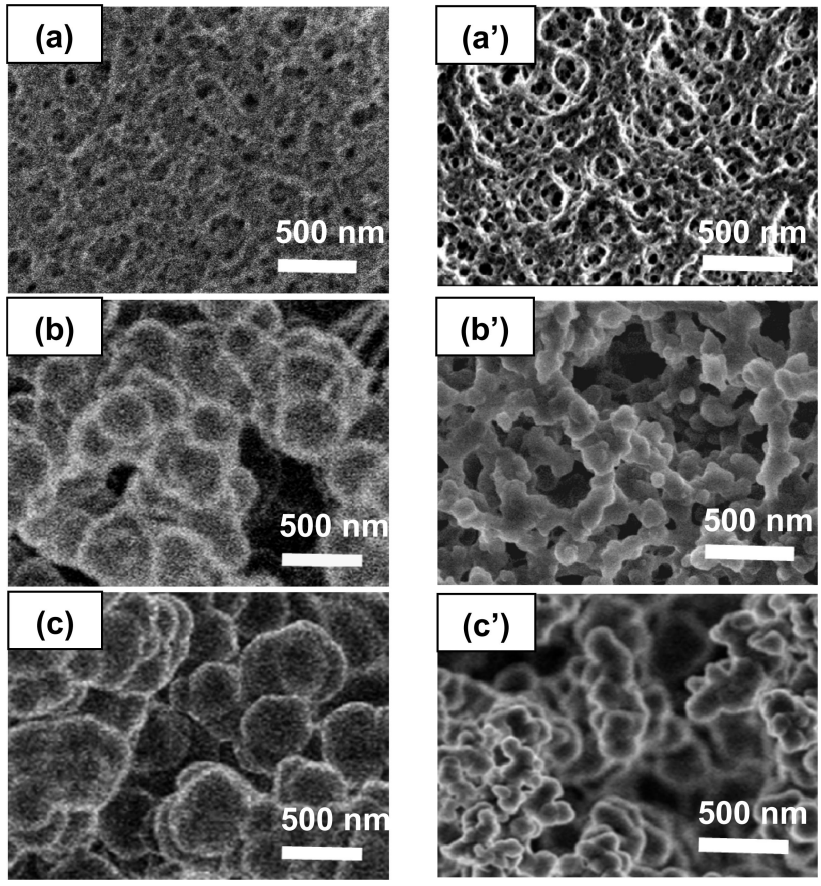

Figure 6. SEM images of poly(GMA-*co*-EGDMA) particles obtained by suspension photopolymerization (left column) and by the microfluidic synthesis (right column) from monomer mixtures comprising (a, a′) DBP, (b, b′) DOP, (c, c,′), and DDP (d, d′). The microfluidic synthesis was conducted as in Figure 4a−d.

incompatibility between the polymer and these porogens, phase separation occurred before the gel point, which facilitated the formation of larger polymer clusters and the formation of a network with larger pore sizes.[2–4]

In order to further examine the advantages of the microfluidic synthesis, we conducted control experiments in which we produced macroporous particles using conventional UV-initiated suspension polymerization. Figure 6 shows typical SEM images of the surfaces of particles obtained by conventional suspension polymerization and by microfluidic means. For all compositions of the reaction mixtures, the microbeads obtained by conventional synthesis had significantly larger size of globules than the particles produced by microfluidic synthesis, especially for the microbeads synthesized by using strongly nonpolar porogens.

4. Discussion

Microfluidic synthesis of macroporous particles resembles suspension polymerization; however, in comparison with conventional suspension polymerization it has two major advantages. First, the distribution of sizes of the macroporous particles synthesized by microfluidic synthesis is significantly narrower than that in conventional suspension polymerization. Narrow polydispersity of particles results from the specific flow-focusing mechanism of monomer emulsification and on-chip polymerization suppresses droplet coalescence. We note that although in the present work we conducted semicontinuous polymerization of the microbeads, on-chip prepolymerization was sufficient to "preshape" the particles and to preserve their narrow size distribution in the consecutive postpolymerization stage.

Second, for the same composition of the reaction mixtures, the size of pores in the particles obtained in microfluidic polymerization was smaller than in the microbeads produced in control experiments using suspension polymerization. To explain this effect, we refer to the results obtained by Svec and Frechet in the synthesis of glycidyl methacrylate-*co*-ethylene dimethacrylate macroporous resins.[24] The authors found that control of the rate of polymerization was an efficient tool in controlling the size of pores: the higher rates of polymerization led to the formation of the larger number of free radicals and, hence, to the larger number of nuclei which aggregated in smaller agglomerates. Apparently, in the microfluidic polymerization, a uniform exposure of every monomer droplet to UV irradiation caused the formation of a greater number of free radicals (compared to conventional suspension photopolymerization) and increased the rate of polymerization. We also note that the uniform exposure of droplets to UV irradiation was also favored by the spinning of the droplets moving through the microchannels.

Along with advantages of microfluidic polymerization, the synthesis of "one particle at a time" raises the concern about the productivity of microfluidic synthesis of macroporous particles. In the present work, the productivity of the individual microfluidic reactor is up to ca. 0.4 g/h (for the flow-focusing emulsification regime) and up to ca. 1 g/h (for the jetting emulsification regime). The productivity of microfluidic polymerization of macroporous particles can be increased by further optimizing the system (e.g., by using more efficient initiators) and by scaling up the production of microbeads in multiple parallel microfluidic reactors. Emulsification and polymerization in parallel microfluidic channels have been recently demonstrated by several research groups.[37–39] In comparison with conventional batch reactions, microreaction synthesis offers two impressive features that are important for the scaled-up production of products: (i) an increase in reaction rates and (ii) the ability to scale up a reaction by merely changing the number of reactors.[40] Future progress in developing a microfluidic technology platform for the synthesis of macroporous polymer particles will be determined by the ability to scale up their production in multiple parallel microreactors in a parallel and highly reproducible manner.

5. Conclusions

Using microfluidic semicontinuous photopolymerization, we synthesized macroporous polymer particles with dimensions from 50 and 100 μm and a well-defined porous structure. The average particle size was controlled by changing the flow rates of the droplet and continuous phases during emulsification of the monomer mixture. The average pore size was controlled by using porogen solvents with different compatibility with the polymer. Particles synthesized by microfluidic synthesis had a notably finer internal structure than the microbeads with the same composition that were produced by conventional suspension polymerization.

Acknowledgment. The authors thank Rohm&Haas Chemicals and Materials Manufacturing Ontario for financial support of this research.

Supporting Information Available: Description of the process of microfabrication of microfluidic reactors, dimensions of microfluidic reactors, and exemplary FTIR spectra. This material is available free of charge via the Internet at http://pubs.acs.org.

References and Notes

(1) Sherrington, D. C. *Chem. Commun.* **1998**, 2275–2286.
(2) Okay, O. *Prog. Polym. Sci.* **2000**, *25*, 711–779.
(3) Okay, O.; Gurun, C. *J. Appl. Polym. Sci.* **1992**, *46*, 421–434.
(4) Horak, D.; Lednicky, F.; Rehak, V.; Svec, F. *J. Appl. Polym. Sci.* **1993**, *49*, 2041–2050.
(5) Paredes, B.; Gonzalez, S.; Rendueles, M.; Diaz, J. M. *Sep. Purif. Technol.* **2004**, *40*, 243–250.
(6) Horak, D.; Svec, F.; Khlal, J.; Adamyan, A.; Volynskii, Y.; Voronkova, O.; Kokov, L.; Gumargalieva, K. *Biomaterials* **1986**, *7*, 467–470.
(7) Horak, D.; Svec, F.; Adamyan, A.; Titova, M.; Voronkova, O.; Trostenyuk, N.; Vishnevskii, V.; Gusienov, E.; Gumergalieva, K. *Clin. Mater.* **1990**, *6*, 287–297.
(8) Horak, D.; Svec, F.; Isakov, Y.; Polyaeva, Y.; Adamyan, A.; Konstantinov, K.; Shafranov, V.; Voronkova, O.; Nikanorov, A.; Trostenyuk, N. *Clin. Mater.* **1992**, *9*, 43–48.
(9) Stegmayr, B. *Transfus. Apher. Sci.* **2005**, *32*, 209–220.
(10) Robert, C. C. R.; Buri, P. A.; Peppas, N. A. *J. Controlled Release* **1987**, *5*, 151–157.
(11) (a) Peters, E. C.; Petro, M.; Svec, F.; Frechet, J. M. J. *Anal. Chem.* **1997**, *69*, 3646–3649. (b) Peters, E. C.; Svec, F.; Frechet, J. M. J. *Adv. Mater.* **1999**, *11*, 1169–1181.
(12) Yu, C.; Xu, M.; Svec, F.; Frechet, J. M. J. *J. Polym. Sci., Part A: Polym. Chem.* **2002**, *40*, 755–769.
(13) Yu, C.; Davey, M. H.; Svec, F.; Frechet, J. M. J. *Anal. Chem.* **2001**, *73*, 5088–5096.
(14) Rohr, T.; Yu, C.; Davey, M.; Svec, F.; Frechet, J. M. J. *Electrophoresis* **2001**, *22*, 3959–3967.
(15) Xie, S.; Allington, R. W.; Frechet, J. M. J.; Svec, F. *Adv. Biochem. Eng./Biotechnol.* **2002**, *76*, 87–125.
(16) Safrany, A.; Beiler, B.; Laszlo, K.; Svec, F. *Polymer* **2005**, *46*, 2862–2871.
(17) Ugelstad, J.; Kaggerud, K. H.; Hansen, F. K.; Berge, A. *Makromol. Chem.* **1979**, *180*, 737–744.
(18) Ugelstad, J.; Söderberg, L.; Berge, A.; Bergström, J. *Nature (London)* **1983**, *303*, 95–96.
(19) Benes, M. J.; Horak, D.; Svec, F. *J. Sep. Sci.* **2005**, *28*, 1855–1875.
(20) Cheng, C. M.; Micale, F. J.; Vanderhoff, J. W.; El-Aasser, M. S. *J. Polym. Sci., Polym. Chem. Ed.* **1992**, *30*, 235–244.
(21) Cheng, C. M.; Vanderhoff, J. W.; El-Aasser, M. S. *J. Polym. Sci., Polym. Chem. Ed.* **1992**, *30*, 245–256.
(22) Li, W-H.; Stover, H. D. H. *J. Polym. Sci., Part A: Polym. Chem.* **1998**, *36*, 1543–1551.
(23) Guiochon, G. *J. Chromatogr. A* **2007**, *1168*, 101–168.
(24) (a) Svec, F.; Hradil, J.; Coupek, J.; Kalal, J. *Angew. Macromol. Chem.* **1975**, *48*, 135–143. (b) Svec, F.; Frechet, J. M. J. *Macromolecules* **1995**, *28*, 7580–7582.
(25) Lloyd, L. L. *J. Chromatogr.* **1991**, *544*, 201–217.
(26) Wernicke, R.; Eisenbeiβ, F. *Chromatographia* **1982**, *15*, 347–350.

(27) Xu, S.; Nie, Z.; Seo, M.; Lewis, P.; Kumacheva, E.; Stone, H. A.; Garstecki, P.; Weibel, D. B.; Gutlin, I.; Whitesides, G. M. *Angew. Chem., Int. Ed.* **2005**, *44*, 724–728.
(28) (a) Seo, M.; Nie, Z.; Xu, S.; Mok, M.; Lewis, P. C.; Graham, R.; Kumacheva, E. *Langmuir* **2005**, *21*, 11614–11622. (b) Nie, Z.; Xu, S.; Mok, M.; Seo, M.; Lewis, P. C. Kumacheva, E. *J. Am. Chem. Soc.* **2005**, *127*, 8058–8063. (c) Lewis, P. C.; Graham, R.; Nie, Z.; Xu, S.; Seo, M.; Kumacheva, E. *Macromolecules* **2005**, *38*, 4536–4538.
(29) Nisisako, T.; Torii, T.; Higuchi, T. *Chem. Eng. J.* **2004**, *101*, 23–29.
(30) Jeong, W. J.; Kim, J. Y.; Choo, J.; Lee, E. K.; Han, C. S.; Beebe, D. J.; Seong, G. H.; Lee, S. H. *Langmuir* **2005**, *21*, 3738–3741.
(31) Xia, Y.; Whitesides, G. M. *Annu. Rev. Mater. Sci.* **1998**, *28*, 153–184.
(32) Anna, S. L.; Bontoux, N.; Stone, H. A. *Appl. Phys. Lett.* **2003**, *82*, 364–366.
(33) *CRC Handbook of Solubility Parameters and Other Cohesion Parameters*, 4th ed.; Barton, A. F. M., Ed.; CRC Press: Boca Raton, FL, 1988; p 62.
(34) Dušek, K. In *Polymer Networks: Structure and Mechanical Properties*; Chompff, A. J., Newman, S., Eds.; Plenum Press: New York, 1971; p 245.
(35) Yang, W.; Hu, J.; Tao, Z.; Li, L.; Wang, C.; Fu, S. *Colloid Polym. Sci.* **1999**, *277*, 446–451.
(36) Fang, D.; Pan, Q.; Rempel, G. L. *J. Appl. Polym. Sci.* **2007**, *103*, 707–715.
(37) Barbier, V.; Willaime, H.; Tabeling, P. *Phys. Rev.* **2006**, *74*, 046306/1–046306/4.
(38) Nisisako, T.; Torii, T.; Takahashi, T.; Takizawa, Y. *Adv. Mater.* **2006**, *18*, 1152–1156.
(39) (a) Li, W.; Nie, Z.; Zhang, H.; Paquet, C.; Seo, M.; Garstecki, P.; Kumacheva, E. *Langmuir* **2007**, *23*, 8010–8014. (b) Li, W.; Young, L.; Nie, Z.; Seo, M.; Garstecki, P.; Simon, C.; Kumacheva, E. *Soft Matter* **2008**, *4*, 258–262.
(40) *Microreactors: New Technology for Modern Chemistry*; Ehrfeld, W., Hessel, V., Lowe, H., Eds.; Wiley-VCH Verlag GmbH: Weinheim, 2000; p 277.

MA800300D